JOURNAL OF SOLID STATE CHEMISTRY 37, 284–293 (1981)

Stability Relations in the Pseudobrookite Solid Solution $Fe_yTi_{3-y}O_5$

IAN E. GREY AND RICHARD R. MERRITT

CSIRO Division of Mineral Chemistry, P.O. Box 124, Port Melbourne, Victoria 3207, Australia

Received June 16, 1980; in final form September 12, 1980

The stability relations in the pseudobrookite solid solution $Fe_yTi_{3-y}O_5$ have been studied in the temperature range 1350–1623°K, using the quench method and controlled gaseous buffers. The temperature/oxygen-fugacity relationships for three univariant assemblages containing the pseudobrookite solid solution have been established, and the composition/temperature curve delineating the pseudobrookite solid solution and its decomposition products has been defined. This curve exhibits two maxima at temperatures of 1413 and 1619°K and corresponding compositions of $FeTi_2O_5$ and $Fe_{0.30}Ti_{2.70}O_5$. The intervening minimum occurs at a temperature of 1339°K and a composition of $Fe_{0.9}Ti_{2.1}O_5$. A qualitative explanation for the shape of the stability curve is given in terms of the relative contributions to the free energy from configurational entropy and enthalpy (internal strain).

Introduction

Members of the pseudobrookite solid-solution series $Fe_yTi_{3-y}O_5$ occur as both terrestrial and lunar minerals. They also appear in the reaction products of the Western Titanium high-temperature ilmenite-beneficiation process (*1*) and the Sorel slag-reduction process (*2*). It was shown in 1967 (*3*) that oxides in the series (hereinafter designated M_3O_5[1]) could be stabilized for all compositions with $0 \leq y \leq 2$, and data published since that time have defined some of the temperature/composition-stability limits for the solid solution. These limits are:

1. The compositions $FeTi_2O_5$ and Fe_2TiO_5 are unstable at temperatures below 1413 and 858°K respectively, and compositions with $1 < y < 2$ become unstable at temperatures between these two values (*5*).

2. All compositions of the solid solution are stable at temperatures above 1623°K (*6*).

3. There is a gap in the solid solution at 1473°K between composition limits of $Fe_{0.75}Ti_{2.25}O_5$ and $Fe_{0.02}Ti_{2.98}O_5$ (*7*).

The present paper reports experimental data that give the composition limits of the miscibility gap in the temperature range 1480–1604°K. In addition, temperature/oxygen-fugacity relationships are given for three univariant three-phase assemblages associated with the miscibility

[1] For consistency with previous terminology (*4*), a solid solution with a pseudobrookite structure is represented by M_3O_5, a solid solution with an ilmenite structure is represented by M_2O_3, a reduced rutile phase is represented by MO_{2-x}, and metallic iron is represented by Fe_m. In this terminology, M indicates iron and/or titanium. For MO_{2-x}, the value of x varies from 0.25 to 0.00. The composition range from $MO_{1.75}$ to $MO_{1.99}$ is spanned by a series of discrete phases whose structures may be considered to derive from the rutile type by crystallographic shear. Between $MO_{1.75}$ and $MO_{1.889}$, the six discrete phases that occur, with the general formula M_nO_{2n-1}, where $n = 4$–9, are known as Andersson–Magneli phases.

0022-4596/81/060284-10$02.00/0

gap. The equilibration-and-quench method was used, and the data were measured in the temperature range 1350–1623°K and the oxygen-fugacity range $10^{-15.4}$–$10^{-11.5}$ atm.

Phase Equilibria Involving M_3O_5

To facilitate discussion of the equilibria in the Fe–Ti–O system, Fig. 1 shows three qualitative phase diagrams for temperatures of 1273, 1403, and 1473°K. These diagrams are based on previously published diagrams in Refs. (*8*), (*9*), and (*7*) respectively, except that Figs. 1a and c show more detail for compositions near the titanium/oxygen boundary and that Fig. 1b is replotted from the original two-triangle diagram for FeO–$FeO_{1.5}$–TiO_2 and FeO–$TiO_{1.5}$–TiO_2.

Both Figs. 1a and c show a single gap in the M_3O_5 solution, but the range of compositions in which the M_3O_5 oxides are unstable is larger at the lower temperature. The gap at 1273°K extends from $Fe_{1.20}Ti_{1.80}O_5$ to effectively Ti_3O_5 (*A* to *E* in Fig. 1a) (*5*), while at 1473°K it extends from $Fe_{0.75}Ti_{2.25}O_5$ to $Fe_{0.02}Ti_{2.98}O_5$ (*D* to *E* in Fig. 1c) (*7*). In addition, different three-phase assemblages exist at the iron-rich end of the gap; at 1273°K the assemblage is M_2O_3 + M_3O_5 + MO_{2-x}, whereas at 1473°K the assemblage is M_3O_5 + MO_{2-x} + Fe_m.

Each diagram in Fig. 1 leads to a unique sequence of equilibrium assemblages when an oxide with a constant [Fe]/[Fe + Ti] ratio is reduced (e.g., along the dashed line *R*–*S*). For this reduction, the assemblages present in the three sequences are listed in Table I. It is apparent from the table that the assemblage M_3O_5 (with composition *C* to *D*) + Fe_m is stable only at temperatures for which the equilibria are those shown in Fig. 1b or c. The minimum temperature for stability of this assemblage was determined to be 1353 ± 10°K by Saha and Biggar (*10*) and 1341°K by Simons and Woermann (*9*). The latter also report that the composition

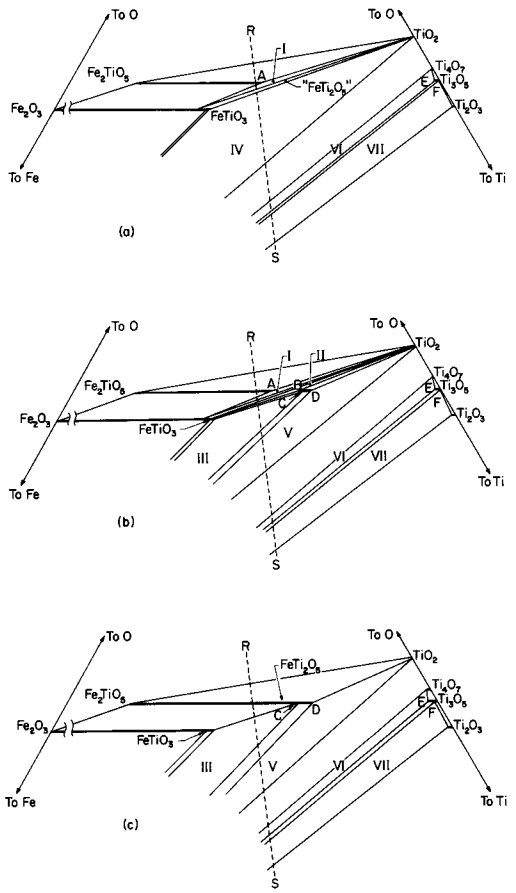

FIG. 1. Qualitative phase diagrams for the Fe–Ti–O system at temperatures of (a) 1273°K, (b) 1403°K, and (c) 1473°K.

of the pseudobrookite phase at 1341°K is close to $Fe_{0.9}Ti_{2.1}O_5$. Since Haggerty and Lindsley (*5*) had reported earlier that $FeTi_2O_5$ decomposes at temperatures below 1413°K, Lindsley (*11*) observed that $FeTi_2O_5$ is stabilized at 1403°K by the addition of either Fe_2TiO_5 or Ti_3O_5. He used the diagram of Simons and Woermann (*9*) to show the equilibria at 1403°K, and it is this figure that is the basis of Fig. 1b, which depicts the phase relations between about 1340 and 1413°K. In contrast to Figs. 1a and c, Fig. 1b shows two gaps in the M_3O_5 solid solution. These gaps occur for compositions ranging from *A* to *B* and from *D* to *E*.

TABLE I

EQUILIBRIUM ASSEMBLAGES THAT OCCUR DURING REDUCTION ALONG LINE R–S IN FIGS. 1a, b, AND c[a]

Univariant three-phase assemblages shown in Fig. 1	Assemblages from Fig. 1a	Assemblages from Fig. 1b	Assemblages from Fig. 1c
	$M_3O_5 + MO_2$	$M_3O_5 + MO_2$	$M_3O_5 + MO_2$
	M_3O_5	M_3O_5	M_3O_5
	$M_3O_5 + M_2O_3$	$M_3O_5 + M_2O_3$	$M_3O_5 + M_2O_3$
I	$M_3O_5(A) + M_2O_3 + MO_2$	$M_3O_5(A) + M_2O_3 + MO_2$	
	$M_2O_3 + MO_2$	$M_2O_3 + MO_2$	
II		$M_3O_5(B) + M_2O_3 + MO_{2-x}$	
		$M_3O_5 + M_2O_3$	
III		$M_3O_5(C) + M_2O_3 + Fe_m$	$M_3O_5(C) + M_2O_3 + Fe_m$
		$M_3O_5 + Fe_m$	$M_3O_5 + Fe_m$
IV	$M_2O_3 + MO_{2-x} + Fe_m$		
V		$M_3O_5(D) + MO_{2-x} + Fe_m$	$M_3O_5(D) + MO_{2-x} + Fe_m$
	$MO_{2-x} + Fe_m$[b]	$MO_{2-x} + Fe_m$[b]	$MO_{2-x} + Fe_m$[b]
VI	$M_3O_5(E) + MO_{2-x} + Fe_m$	$M_3O_5(E) + MO_{2-x} + Fe_m$	$M_3O_5(E) + MO_{2-x} + Fe_m$
	$M_3O_5 + Fe_m$	$M_3O_5 + Fe_m$	$M_3O_5 + Fe_m$
VII	$M_3O_5(F) + M_2O_3 + Fe_m$	$M_3O_5(F) + M_2O_3 + Fe_m$	$M_3O_5(F) + M_2O_3 + Fe_m$

[a] The letters A through F refer to the M_3O_5 compositions shown in Fig. 1.

[b] $MO_{2-x} + Fe_m$ is used to describe a series of two- and three-phase regions in which reduced rutile phases coexist with metallic iron.

Experimental

Phase equilibria were determined by the equilibration-and-quench method. That is, samples (in pellet form) were heated in a controlled atmosphere at the required temperature for a minimum of 6 hr; they were then quenched with liquid nitrogen and their phases were determined by X-ray diffraction. The samples were prepared from mixtures of Fe_2O_3 and the anatase form of TiO_2 (both certified Fischer reagents) that had been dried at 1073°K prior to mixing. The following two precautions were observed to ensure that equilibrium was achieved and that the phase boundaries were positioned as accurately as the experimental technique would allow:

1. Two samples were heated at a time. One of these samples consisted of the oxides as mixed so that equilibrium was approached by reduction. The other sample consisted of mixed oxides that had been prereduced at an oxygen fugacity low enough to stabilize a more reduced phase assemblage than the required one. Thus, in this sample, equilibrium was approached by oxidation.

2. The quenched samples were ground and reheated until successive heatings produced no changes in their X-ray-diffraction patterns.

The oxygen fugacity was controlled by mixing hydrogen and carbon dioxide in ratios established by metering the gases through calibrated flowmeters. The fugacity was calculated from the H_2/CO_2 ratio, using the computer program CHEMIX (*12*) and basic thermodynamic data consistent with that in the JANAF thermochemical tables (*13*).

The samples were heated, inside a recrystallized alumina tube, by a platinum resistance furnace. Their temperatures were measured with a Pt/Pt–13%Rh thermocouple that was located on the outside wall of the tube. This external thermocouple was calibrated (as a function of temperature and H_2/CO_2 ratio) against a similar thermocouple that was located inside the tube at the position of the samples. Uncertainties resulting from the use of a tempera-

ture-measuring potentiometer, from furnace instability, and from thermocouple calibration are estimated to limit the precision of the sample-temperature measurements to ±2°K. A possible thermocouple inaccuracy of ±0.5% (*14*) leads to an uncertainty of ±6°K at the highest experimental temperature (1623°K). Possible errors resulting from instability in the H_2/CO_2 ratio, from calibrating and reading the flowmeters, and from impurities in the equilibrating gases lead to an uncertainty of ±0.05 in $\log f_{O_2}$. The thermochemical data (*13*) used to calculate the oxygen fugacity lead to an additional uncertainty of ±0.03 in $\log f_{O_2}$. All together, these figures suggest errors of up to ±8°K in the measured sample temperatures and up to ±0.08 in $\log f_{O_2}$.

The X-ray diffraction patterns were obtained with a Philips diffractometer fitted with a graphite monochromator, using Cu$K\alpha$ radiation.

Results

Univariant Equilibria Involving M_3O_5

The first part of the experimental program determined the temperature/oxygen-fugacity relationships for three univariant assemblages that have M_3O_5 as a component phase. These assemblages are II, V, and VI in Table I. The data were measured at the fixed ratio [Fe]/[Fe + Ti] = 0.394, which is shown in Figs. 1a, b, and c by the dashed line R–S. This ratio was chosen for two reasons:

1. The ratio is typical of Western Australian altered ilmenite, so the experimental results are applicable to the Western Titanium ilmenite-beneficiation process (*1*).

2. The ratio ensured that the minor phases at the three phase boundaries always appeared in easily detectable amounts.

Data was measured at temperatures between 1350 and 1623°K and at oxygen fugacities between $10^{-15.0}$ and $10^{-11.5}$ atm. The results are shown in Fig. 2. Also shown in Fig. 2 are the data of Simons and Woermann (*9*) at 1403°K, together with the results of the present authors (*4*) for the univariant assemblages III and V at temperatures below 1493°K (i.e., at values of $1/T$ greater than 0.67×10^{-3}°K^{-1}). Figure 2 gives 1619 ± 8°K as the minimum temperature for complete solid solution, and at that temperature the oxygen fugacity for the assemblage $M_3O_5 + MO_{2-x} + Fe_m$ (V and VI in Table I) is $10^{-12.9\pm0.2}$ atm. The linearly extrapolated curves for the univariant assemblages II, III, and V meet at a point that defines the minimum temperature for the existence of M_3O_5 in equilibrium with Fe_m. This intersection occurs at 1339 ± 8°K ($1/T = 0.7468 \times 10^{-3}$°$K^{-1}$) and $10^{-14.96\pm0.08}$ atm. Experimental gas-metering limitations did not allow the oxygen fugacity to be increased enough to cross the second gap in the M_3O_5 solid solution in order to record data for assemblage I.

Composition Limits for M_3O_5

The second part of the experimental program determined, for a series of temperatures, the compositions of the M_3O_5 phases in the assemblages $M_3O_5 + MO_{2-x} + Fe_m$ (V and VI in Table I). The technique consisted of heating oxide mixtures with different [Fe]/[Fe + Ti] ratios at the conditions marked with crosses in Fig. 2 and determining the phases in the quenched samples. The conditions under which the samples were heated, their [Fe]/[Fe + Ti] ratios, and the phases found in them after quenching are given in Table II. The fact that the experimental conditions were close to those of the three-phase assemblage $M_3O_5 + MO_{2-x} + Fe_m$ was confirmed by reheating four sets of samples at conditions that lie within the two-phase region $MO_{2-x} + Fe_m$ (see Fig. 2). These reheatings generally gave the expected $MO_{2-x} + Fe_m$ phases. However, in assemblage VI and in samples

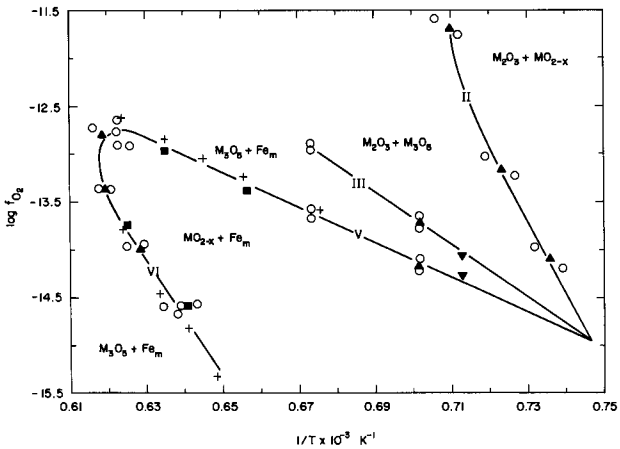

FIG. 2. Experimentally determined phase relations for the Fe–Ti–O system. The circles indicate the presence of two phases in the quenched samples, while the upright triangles indicate the presence of three phases. The inverted triangles indicate the temperature and oxygen-fugacity conditions for the existence of assemblages III and V, as reported by Simons and Woermann (*11*). The crosses indicate the heating conditions for the samples that were used to define the composition limits of the miscibility gap (*D* to *E* in Fig. 1c). The squares indicate the heating conditions for the samples that were used to confirm that the composition limits were defined near the three-phase assemblages V and VI. The graph includes the results of the present authors (*4*) for assemblages III and V. The equilibrations were performed for the ratio [Fe]/[Fe + Ti] = 0.394 (see Fig. 1).

with an [Fe]/[Fe + Ti] ratio of less than 0.1, the M_3O_5 phase was still present after reheating. This was not the case for samples with higher [Fe]/[Fe + Ti] ratios; in them the M_3O_5 phase always disappeared upon reheating.

The data given in Table II can be interpreted using Fig. 1c. In a series of oxides heated to determine the M_3O_5 composition in assemblage V (i.e., composition *D* in Fig. 1c), those mixtures that are richer in iron than composition *D* will give the equilibrium assemblage M_3O_5 + Fe_m, and those that are poorer in iron will give the assemblage M_3O_5 + MO_{2-x}. Similarly, for the M_3O_5 composition in assemblage VI (i.e., composition *E* in Fig. 1c), those mixtures with more iron than composition *E* will give M_3O_5 + Fe_m in equilibrium, while those poorer in iron will give M_3O_5 + MO_{2-x}. The MO_{2-x} phase in the latter case will be M_4O_7.

The above approach was used to determine the M_3O_5 compositions shown in Fig. 3. The experimental data in this graph are shown by error bars drawn parallel to the composition axis, and they are combined with published data (*5, 7, 9*) to define the shape of the stability curve for M_3O_5 in the temperature range 1150–1619°K.

Discussion

Temperature/Oxygen-Fugacity Relationships

The experimental results show that the gap (*D* to *E*) in the M_3O_5 solution closes at a temperature of 1619 ± 8°K and an oxygen fugacity of $10^{-12.9\pm0.2}$ atm. This temperature is consistent with the result of Grey and Ward (*6*), who suggest that the solid solution is complete above 1623°K. The large uncertainty in the oxygen fugacity is a consequence of the curvature of the lines in Fig. 2 that represent the assemblage M_3O_5 + MO_{2-x} + Fe_m (V and VI). The measured data are consistent with those of Simons

TABLE II

RESULTS OF THE STUDY OF THE COMPOSITION OF THE M_3O_5 PHASE IN THE ASSEMBLAGE M_3O_5 + MO_{2-x} + Fe_m[a]

Temperature (°K)	Log f_{O_2}	[Fe]/[Fe + Ti] ratio	Phases present[b]		
			M_3O_5	MO_{2-x}	Fe_m
1542	−15.329	0.0167	S	S	—
		0.0333	S	—	T
		0.0500	S	—	S
		0.0667	S	—	S
1559	−14.937	0.0167	S	S	—
		0.0333	S	—	T
		0.0500	S	—	T
		0.0667	S	—	S
1578	−14.476	0.0167	T	S	—
		0.0333	S	—	—
		0.0500	S	—	T
		0.0667	S	—	S
1602	−14.012	0.0167	S	S	—
		0.0333	S	—	—
1602	−14.002	0.0167	T	S	—
		0.0333	S	T	—
		0.0500	S	—	T
		0.0667	S	—	T
1604	−12.637	0.1833	S	—	T
1603	−12.654	0.1666	S	—	—
		0.2000	S	—	S
		0.2333	S	—	S
1575	−12.851	0.1833	S	—	—
1574	−12.886	0.1666	S	T	—
		0.2000	S	—	T
		0.2333	S	—	S
1553	−13.003	0.2000	S	—	—
		0.2333	S	—	S
1551	−13.047	0.1666	S	S	—
		0.1833	S	—	—
		0.2167	S	—	S
1526	−13.240	0.1833	S	T	—
		0.2000	S	T	—
		0.2167	S	—	—
		0.2333	S	—	S
1480	−13.590	0.2167	S	T	—
		0.2333	S	T	—
		0.2500	S	—	—
		0.2666	S	—	T

[a] The braces indicate paired groups of data that were used to define single error bars in Fig. 3.

[b] Phases present in substantial amounts are shown by the letter S, phases present in trace amounts by the letter T.

and Woermann (*9*) at their lower temperature. However, at 1573°K they encountered the metastable assemblage M_3O_5 + MO_{2-x} + Fe_m between oxygen fugacities of $10^{-12.85}$ and $10^{-12.14}$ atm, whereas the present results show that this stable assemblage at

1573°K occurs at $10^{-12.95\pm0.08}$ atm (V in Fig. 2). Similar metastable assemblages were found in the present study in samples that were heated only once; equilibrium was generally achieved on reheating.

Extraopolation of the curves representing equilibrium assemblages II, III, and V indicates that the minimum temperature for existence of the assemblage M_3O_5 + Fe_m is 1339 ± 8°K at an oxygen fugacity of $10^{-14.95\pm0.08}$ atm. This invariant temperature agrees with our earlier result (*4*), with the 1341°K reported by Simons and Woermann (*9*), and (within the combined error limits) with the 1353 ± 10°K reported by Saha and Biggar (*10*). The present value for the oxygen fugacity of this invariant point is also consistent with the value of $10^{-15.15\pm0.20}$ atm given by these latter authors.

It was not possible to measure equilibrium data for assemblage I, M_2O_3 + M_3O_5 + MO_{2-x}, so the conditions at the peak of the gap *A* to *B* are not defined. The maximum temperature for the assemblage M_2O_3 + M_3O_5 + MO_{2-x} from Fig. 2 is 1416°K, a value that is very close to the 1413 ± 10°K given by Haggerty and Lindsley (*5*) for the decomposition of $FeTi_2O_5$. The two sets of data are consistent if the conditions at the top of curve II in Fig. 2 are very close to those of the maximum in the gap *A* to *B*. It is therefore proposed that this gap closes at about 1416°K and $10^{-11.8}$ atm.

Composition/Temperature Relationships

In Fig. 3, the experimental data are shown by error bars centered on the M_3O_5 limit compositions as determined from the data in Table II. The lengths of these error bars, [Fe]/[Fe + Ti] = 0.0167, equal the composition increments between the heated samples and indicate the major compositional error in defining the gap *D* to *E*. The compositions lettered *A* to *E* in Fig. 3 correspond to the similarly lettered compositions in Fig. 1. A smaller uncertainty

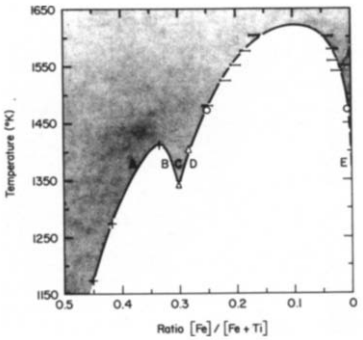

FIG. 3. The ratio [Fe]/[Fe + Ti] in the M_3O_5 solution as a function of temperature for the pseudobrookite solid solution $Fe_yTi_{3-y}O_5$. The results of the present study are shown by error bars, those of Simons and Woermann (*11*) by triangles, those of Haggerty and Lindsley (*5*) by crosses, and those of Grey *et al.* (*7*) by circles. The shaded area represents the region where M_3O_5 is stable.

results from heating at conditions displaced from the three-phase boundary (see the crosses in Fig. 2). The error introduced by this displacement is estimated to be less than 0.005 in the ratio [Fe]/[Fe + Ti].

Figure 3 shows that for temperatures between 1413 and 1619 ± 8°K, there is only one gap in the M_3O_5 solution, and it is for this range that the phase relations are those shown in Fig. 1c. Because of the flatness of the maximum of the curve defining this gap, the [Fe]/[Fe + Ti] ratio in the oxides at the maximum temperature cannot be specified more precisely than 0.10 ± 0.02. The M_3O_5 phase corresponding to this ratio is $Fe_{0.30}Ti_{2.70}O_5$.

Between 1339 and 1413°K there are two gaps in the M_3O_5 solid solution; the widths of these gaps increase as the temperature decreases. The temperature 1339 ± 8°K corresponds to the point in Fig. 1b at which the M_3O_5 compositions *B*, *C*, and *D* become the same and below which the equilibrium phase relations are those depicted in Fig. 1a, where there is only one gap. This single gap below 1339°K occurs for compositions between *A* and *E*, and from the data of Haggerty and Lindsley (*5*), the [Fe]/[Fe +

Ti] ratios at A are always greater than 0.33. Simons and Woermann (*9*) give the [Fe]/[Fe + Ti] ratio at 1339°K, where B, C, and D coalesce, as 0.3.

Entropy Stabilization

Navrotsky (*15*) shows that although many compounds with a pseudobrookite structure have an endothermic heat of formation from the oxides M_2O_3 and TiO_2, they are stabilized at high temperatures by a large positive entropy term. She considers that the disordering of different cations on the two crystallographically independent sites in the pseudobrookite structure is a major contributor to the stabilizing entropy. Mössbauer studies led Reid and Ward (*16*) to conclude that the Fe_2TiO_5–Ti_3O_5 solid solution can best be described as two solutions. The first, for compositions between Fe_2TiO_5 and $FeTi_2O_5$, contains the cations Fe^{3+}, Fe^{2+}, and Ti^{4+}; the second, for compositions between $FeTi_2O_5$ and Ti_3O_5, contains the cations Fe^{2+}, Ti^{3+}, and Ti^{4+}. From Reid and Ward's model, the stabilizing configurational entropy would be at a minimum at the composition in which only Fe^{2+} and Ti^{4+} cations occur, namely $FeTi_2O_5$. It is this oxide that has the minimum stability in the region A to B.

The standard formula for evaluating the ideal entropy of mixing (*17*) was used by Waldbaum (*18*) to estimate the configurational entropy of solid solutions. He determined the ideal entropy of mixing the cations on each cation site and then summed over all the sites; that is,

$$\Delta S \text{ (configurational)} = -R \sum_{ij} N_{ij} \ln N_{ij},$$

where R is the gas constant and N_{ij} is the atom fraction of cation i on cation site j. This formula is applied to the solution $Fe_{1-a}Ti_{2+a}O_5$, using the data of Grey and Ward (*6*) for the Fe^{2+} occupancy of 4*c* and 8*f* sites, and assuming that the Ti^{3+} is randomly distributed over all titanium sites.

The calculated configurational entropy per mole of M_3O_5 is plotted against composition parameter $1 - a$ in Fig. 4. The assumed Ti^{3+} distribution is consistent with the view of Asbrink and Magneli (*19*) that the formal valency of all metal atoms in high-temperature Ti_3O_5, a solution end number, is $3\frac{1}{3}$. The proposed cation-distribution model leads to ideal configurational entropies for $FeTi_2O_5$ and $Fe_{0.9}Ti_{2.1}O_5$ of 11.7 and 16.9 J $mole^{-1}$ °K^{-1}. Thus, at 1339°K the addition of 0.1 mole of Ti_3O_5 to $FeTi_2O_5$ stabilizes the M_3O_5 structure by 7 kJ $mole^{-1}$.

The Gap D to E in the M_3O_5 Solid Solution

The reaction that controls the formation of this gap is

$$(1 - a)\text{Fe} + \frac{2 + a}{n} \text{Ti}_n\text{O}_{2n-1} + \left[\frac{5}{2} - \frac{(2n - 1)(2 + a)}{2n}\right] \text{O}_2 = \text{Fe}_{1-a}\text{Ti}_{2+a}\text{O}_5,$$

in which the very small incorporation of iron in the Ti_nO_{2n-1} (*20*) phases is ne-

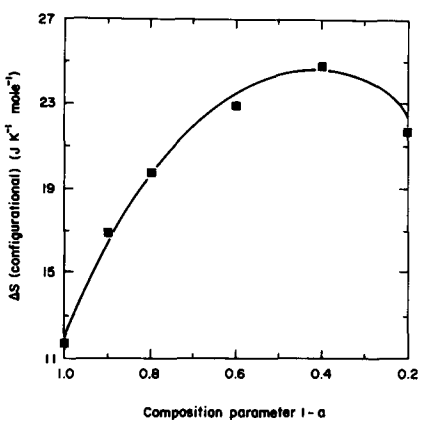

FIG. 4. Calculated configurational entropy as a function of composition for the solid solution $Fe_{1-a}Ti_{2+a}O_5$.

glected. At equilibrium (i.e., at conditions of temperature and composition corresponding to a point on the curve D to E in Fig. 3),

$$\frac{2+a}{n}\Delta G_{f_{M_nO_{2n-1}}} = \Delta G_{f_{M_3O_5}},$$

where ΔG_f is the free energy of formation per mole. This equilibrium can be expressed as

$$T_{eq} = \frac{\Delta H_{f_{M_3O_5}} - \frac{2+a}{n}\Delta H_{f_{M_nO_{2n-1}}}}{\Delta S_{f_{M_3O_5}} - \frac{2+a}{n}\Delta S_{f_{M_nO_{2n-1}}}} = \frac{\Delta(\Delta H_f)}{\Delta(\Delta S_f)}, \quad (1)$$

where T_{eq} is the equilibrium temperature corresponding to the [Fe]/[Fe + Ti] ratio in $Fe_{1-a}Ti_{2+a}O_5$, ΔH_f is the enthalpy of formation per mole, and ΔS_f is the entropy of formation per mole.

The results given in Fig. 3 show that T_{eq} is increased by the addition of Ti^{3+} to $Fe_{0.9}Ti_{2.1}O_5$ until the composition $Fe_{0.30}Ti_{2.70}O_5$ is reached. From Eq. (1), this experimental result may be explained by an increase in $\Delta(\Delta H_f)$, a decrease in $\Delta(\Delta S_f)$, or both. If the first case is dominant, it implies that the strain enthalpy of introducing extra shear phases to accommodate the extra reduction in reduced rutiles increases less rapidly than the strain enthalpy arising from the incorporation of Ti^{3+} into the M_3O_5 solution. A significant strain-enthalpy contribution to the destabilization of M_3O_5 is consistent with the onset, at [Fe]/[Fe + Ti] $\simeq$ 0.117, of the monoclinic distortion in the M_3O_5 solution (*6*) occurring close to the maximum of the stability curve. This distortion, which increases as the [Fe]/[Fe + Ti] ratio decreases below 0.117, probably reduces the strain that arises from the tendency of reduced titanium to form metal-to-metal bonds. In terms of Eq. (1), the monoclinic distortion would reduce the rate at which $\Delta H_{f_{M_3O_5}}$ increases as reduced titanium is incorporated into the M_3O_5 phase, thus leading to a decrease in T_{eq} in agreement with the experimental results.

The above argument cannot exclude some decrease in $\Delta(\Delta S_f)$ as a cause for the increase in T_{eq} from $Fe_{0.9}Ti_{2.1}O_5$ to $Fe_{0.3}Ti_{2.7}O_5$, since it is based on the assumption that the monoclinic distortion seen in the quenched samples occurs in the M_3O_5 solution at equilibrium temperatures. Without more complete knowledge of the high-temperature equilibria, it is not possible to fully assess the relative importance of either the entropy term or the enthalpy term in determining the value of T_{eq}.

Conclusions

Phase relations in the Fe–Ti–O system were studied under controlled oxygen fugacities at temperatures betwen 1350 and 1623°K.[2] The experimental results are combined with data from the literature to define the temperature/composition relation for the stability of the M_3O_5 solid solution. The following conclusions are drawn:

1. The minimum temperature for complete solid solution in the solution Fe_2TiO_5–Ti_3O_5 is 1619 ± 8°K.

2. A single asymmetric gap exists in the M_3O_5 solid solution from 1413 to 1619°K. The oxygen fugacity is $10^{-12.9\pm0.2}$ atm at the maximum temperature, and the [Fe]/[Fe + Ti] ratio in the oxide phase is 0.10 ± 0.02.

3. Between 1339 and 1413°K, there are two gaps in the M_3O_5 solid solution. The

[2] It was brought to the authors' attention by one of the journal referees that a closely related study of stability relations in the pseudobrookite solid solution had recently been carried out at the Technische Hochschule Aachen (*21*). Although different experimental techniques were used (closed systems with subsequent X-ray and chemical analyses), the results are consistent with those reported here.

second gap is close to symmetrical about the composition $FeTi_2O_5$.

4. Extrapolation of the experimental data gives the conditions 1339 ± 8°K and $10^{-14.96\pm0.08}$ atm for the invariant point at the minimum of the dip in the stability curve. Published data show that the composition of the solution at these conditions has the ratio [Fe]/[Fe + Ti] = 0.3 (i.e., the oxide $Fe_{0.9}Ti_{2.1}O_5$).

5. The increased stability of the $Fe_{0.9}Ti_{2.1}O_5$ relative to $FeTi_2O_5$ is explained in terms of the increased configurational entropy in the former phase caused by the addition of Ti^{3+} cations to the $FeTi_2O_5$ phase, which ideally contains only Fe^{2+} and Ti^{4+}.

6. The shape of the stability curve *DE* is considered in terms of the energy balance between the configurational entropies and the lattice strains of the oxides in equilibrium in this region, namely, MO_{2-x} and M_3O_5.

Acknowledgments

The authors wish to acknowledge Drs. F. R. A. Jorgensen and A. G. Turnbull of the CSIRO Division of Mineral Chemistry for their helpful and constructive criticisms of the manuscript.

References

1. B. F. Bracanin, P. W. Cassidy, J. M. Mackay, and H. W. Hockin, T.M.S. Paper Selection No. A72-31, 309 (1972).
2. S. A. Forman, A. T. Prince, and N. F. H. Bright, "Research Investigation of the Mines Branch," Research Report No. MD-169, Department of Mines and Technical Surveys, Canada (1954).
3. G. Asbrink and A. Magneli, *Acta Chem. Scand.* **21**, 1977 (1967).
4. I. E. Grey and R. R. Merritt, *J. Solid State Chem.* **32**, 41 (1980).
5. S. E. Haggerty and D. H. Lindsley, *Carnegie Inst. Washington Yearb.* **68**, 247 (1970).
6. I. E. Grey and J. Ward, *J. Solid State Chem.* **7**, 300 (1973).
7. I. E. Grey, A. F. Reid, and D. G. Jones, *Inst. Mining Met. Trans. Sect. C* **83**, 105 (1974).
8. R. R. Merritt and A. G. Turnbull, *J. Solid State Chem.* **10**, 252 (1974).
9. B. Simons and E. Woermann, *Contrib. Mineral. Petrol.* **66**, 81 (1978).
10. P. Saha and G. M. Biggar, *Indian J. Earth Sci.* **1**, 43 (1974).
11. D. H. Lindsley, *in* "Oxide Minerals" (D. Rumble III, Ed.), Mineralogical Society of America Short Course Notes, Vol. 3 (November 1976).
12. A. G. Turnbull, *in* "APCOM 77," p. 49, Australasian Inst. Mining & Metallurgy, Melbourne (1977).
13. D. R. Stull and H. Prophet, "JANAF Thermochemical Tables," 2nd ed., Nat. Bureau of Stand., Washington, D.C. (1971).
14. "1970 Annual Book of ASTM Standards," part 30, p. 669, Amer. Soc. for Testing and Materials, Philadelphia (1970).
15. A. Navrotsky, *Amer. Mineral.* **60**, 249 (1975).
16. A. F. Reid and J. C. Ward, *Acta Chem. Scand.* **25**, 1475 (1971).
17. K. S. Pitzer and L. Brewer, *in* "Thermodynamics," 2nd ed., p. 226, McGraw–Hill, New York (1961).
18. D. R. Waldbaum, *Contrib. Mineral. Petrol.* **39**, 33 (1973).
19. S. Asbrink and A. Magneli, *Acta Crystallogr.* **12**, 575 (1959).
20. I. E. Grey, C. Li, and A. F. Reid, *J. Solid State Chem.* **11**, 120 (1974).
21. A. Ender, R. Hofmann, L. Stapper, G. Dhupia, and E. Woermann, *Fortschr. Mineral.* **58**, 26 (1980).